Shaffer, A. G., and C. E. Hamrin, "Enzyme Separation by Parametric Pumping," *AIChE J.*, **21**, 782 (1975).
Shendalman, L. H., and J. E. Mitchell, "A Study of Heatless Absorption in the Model System $CO_2$ in He," *Chem. Eng. Sci.*, **27**, 1449 (1972).
Sweed, N. H., and R. A. Gregory, "Parametric Pumping: Modeling Direct Thermal Separations of Sodium Chloride-Water in Open and Closed Systems," *AIChE J.*, **17**, 171 (1971).
Sweed, N. H., and J. Rigaudeau, "Equilibrium Theory and Scale-Up of Parametric Pumps," *AIChE Symposium Ser. No. 152*, p. 1 (1975).
Turnock, P. H., and R. H. Kadlec, "Separation of Nitrogen and Methane Via Periodic Adsorption," *AIChE J.*, **17**, 335 (1971).
Weaver, K., and C. E. Hamrin, "Separation of Hydrogen Isotopes by Heatless Adsorption," *Chem. Eng. Sci.*, **29**, 1873 (1974).
Wilhelm, R. H., A. W. Rice, and A. R. Bendelius, "Parametric Pumping: A Dynamic Principle for Separating Fluid Mixtures," *Ind. Eng. Chem. Fundamental*, **5**, 141 (1966).
Wilhelm, R. H., and N. H. Sweed, "Parametric Pumping: Separation of Mixture of Toluene and n-Heptane," *Science*, **159**, 522 (1968).
Wilhelm, R. H., A. W. Rice, D. W. Rolke, and N. H. Sweed, "Parametric Pumping," *Ind. Eng. Chem. Fundamental*, **7**, 337 (1968).

*Manuscript received January 14, 1977; revision received June 20, and accepted June 27, 1977.*

# Dispersed Phase Mass Transfer During Drop Formation Under Jetting Conditions

A recent design procedure for perforated plate extraction columns requires extension to include jetting conditions at each perforation. For this purpose, correlations are obtained for jet length, jet contraction, drop size, and mass transfer coefficients in disperse phase controlled liquid-liquid systems. Experimental variables include nozzle size, flow velocity, and physical properties.

**A. H. P. SKELLAND**
**and**
**Y-F HUANG**
**Chemical Engineering Department**
**The University of Kentucky**
**Lexington, Kentucky 40506**

## SCOPE

A rate approach to the complete design of perforated plate extraction columns was recently published by Skelland and Conger (1973). This provisional procedure uses rate equations describing mass transfer during droplet formation, rise, and coalescence and incorporates relevant hydrodynamics to locate a pseudoequilibrium curve. This curve is used in place of the true equilibrium relationship when stepping off the necessary number of actual stages between the pseudoequilibrium and operating curves on the x-y diagram. The provisional procedure was written in Fortran IV computer language, by W. L. Conger, and his complete computer program is given by Skelland (1974). The print-out gives the number of real plates required for a prescribed separation, the number of perforations per plate, the column diameter, and the cross-sectional area of the downcomers. Substantial agreement was found between predictions and all appropriate data in the published literature.

The design procedure just described is limited to operations in which drops form and detach at the perforations on each plate. Mayfield and Church (1952), however, have shown that plate efficiency increases substantially (in some cases 2½ fold) when drops are formed at the ends of liquid jets issuing from the perforations. Column throughput rates are also much higher under such conditions.

This study was accordingly undertaken to extend the above design procedure to columns operating with the benefits of drop formation under jetting conditions. Correlations were sought for jet length, jet contraction, drop size, and mass transfer coefficients in disperse phase controlled liquid-liquid systems. Variables included nozzle size, flow velocity, and physical properties, and photographic techniques were used to determine drop and jet characteristics.

## CONCLUSIONS AND SIGNIFICANCE

The length of a liquid jet issuing from a hole or nozzle on a perforated plate in extraction under jetting conditions has been correlated in Equation (27) of the present paper. The expression is confined to flow rates up to the maximum jet length and to systems with high interfacial tension. The contraction at breakup of a liquid jet undergoing mass transfer to another liquid agrees quite well with that for a jet without mass transfer; the jet diameter at breakup is correlated here in Equation (28). Equation (29) correlates the size of drops formed from jet breakup in the presence of mass transfer to the surrounding liquid.

The mass transfer aspects of this work have shown that correlations of coefficients for mass transfer during drop formation, free fall, and coalescence obtained under nonjetting conditions can be extended to the jetting region with success. The assumption of cone-parabolic flow in the liquid jet gave slightly better predictions of mass transfer rate than did the penetration theory. Good agreement

was obtained between experimental and predicted total mass transfer rates, compounded from those during jet flow, drop formation, free fall, and coalescence.

These results permit the aforementioned design procedure for perforated plate extraction columns to be extended to operation under jetting conditions, at least for disperse phase controlled systems. Combination with work currently proceeding on continuous phase controlled systems should enable the formulation of more comprehensive design methods.

The design procedure recently published by Skelland and Conger (1973) for liquid-liquid extraction in perforated plate columns uses a phenomenological approach, and its continued development should be useful both for the design of new processes and for predicting the results of modifying the operation of existing equipment.

When the velocity of the dispersed phase through the perforated plate exceeds the jetting velocity, a jet issues from each perforation, breaking into drops at some distance from the plate. Mayfield and Church (1952) found experimentally that extraction rates are substantially higher under jetting than nonjetting conditions. Unfortunately, quantitative relationships for mass transfer during drop formation under jetting conditions are nonexistent. This study was therefore undertaken to measure and correlate the mass transfer rate under jetting conditions, using experimental and computational techniques similar to those of Skelland and Minhas (1971) for drop formation at nonjetting velocities, but using only one nozzle. Systems that are dispersed phase controlled were used throughout.

The results will enable extension of the above design procedure to columns operating with the benefits of drop formation arising from jet breakup.

## LITERATURE REVIEW

For perforated plate extraction columns operated under jetting conditions, there are four stages of mass transfer occurring between any two consecutive plates: in the liquid jet, during drop formation, during drop free fall (or rise), and during drop coalescence at the next plate. To predict the rate of mass transfer at each stage, one has to know the physical dimensions of the liquid jet and the size of drops formed from the jet breakup.

### Characteristics of Liquid Jet Flow

*Jet Length.* Many attempts have been made to predict the jet length under non-mass-transfer conditions. Important contributions include those of Rayleigh (1879, 1879), Smith and Moss (1917), Tyler and Richardson (1925), Weber (1931), Tyler and Watkin (1932), Tomotika (1935), Grant and Middleman (1966), and Meister and Scheele (1967, 1969).

The latter workers (Meister and Scheele, 1969) measured jet lengths during the transfer of acetone between benzene jets and water. They found that transfer in both directions was stabilizing relative to the non-mass-transfer case and that transfer into the jet produced significantly longer jets than transfer out.

Sawistowski (1973), in contrast, noted that jet breakup in liquid-liquid systems is accelerated by mass transfer into a jet (if $d\sigma/dC_A < 0$) and decelerated by transfer out.

Burkholder and Berg studied the effect of mass transfer on laminar jet breakup for liquid jets in gases (1974) and liquid jets in liquids (1974). For the latter case, they predicted mass transfer of a surface tension lowering solute either into or out of the jet may be either stabilizing (longer jets) or destabilizing (shorter jets), depending on physical properties of the system and the mass transfer rate.

*Jet Contraction.* It is known experimentally that the diameter of a Newtonian jet contracts with increasing distance from the nozzle. Christiansen and Hixson (1957) correlated jet contraction at the flow rate corresponding to minimum drop size after breakup in liquid-liquid systems by using the concept of a reduced nozzle diameter, defined as the ratio of nozzle diameter to a system length parameter $l_s$. They found a relationship for jet contraction in a plot of $d_n/d_{jc}$ vs. $d_n/l_s$. Skelland and Johnson (1974) followed the concept of reduced diameter and constructed a similar plot to that of Christiansen and Hixson (1957) for various jetting conditions. They found reasonable correlation over a range of flow rates through the nozzle.

*Jetting Velocity.* Scheele and Meister (1968) considered the mechanism of liquid jet formation in liquids. They reasoned that a jet will form if there is sufficient upward force at the nozzle exit. For a dispersed phase with parabolic velocity distribution in the nozzle, they find

$$U_{nj} = 1.73 \left[ \frac{\sigma}{\rho_d d_n} \left( 1 - \frac{d_n}{d_f} \right) \right]^{1/2} \tag{1}$$

where $d_f$ is the diameter of the drop that would form at the nozzle velocity $U_{nj}$ if a jet did not appear. For plug flow in the nozzle the constant, 1.73, is replaced by 2.0.

*Drop Size from Jet Breakup.* Keith and Hixson's study in liquid-liquid systems (1955) indicated that the drop volume passes through a minimum when plotted against the dispersed phase flow rate. Drops of minimum size of course correspond to maximum interfacial area.

Siemes and Kauffman (1957) showed in their experimental work on liquid-liquid systems that the most important parameters controlling drop size were the nozzle diameter, injection velocity, interfacial tension, and the density difference between the phases.

From a study of the disintegration of organic liquid jets in a continuum of water, Christiansen and Hixson were able to correlate the nozzle velocity $U_{nm}$ at which the minimum drop size occurs with the system properties. Their results were put in the following form by Treybal (1963):

$$U_{nm} = 2.69 \left( \frac{d_{jm}}{d_n} \right)^2 \left( \frac{\sigma/d_{jm}}{0.5137\,\rho_d + 0.4719\,\rho_c} \right)^{0.5} \tag{2}$$

where the ratio of nozzle-to-jet diameter is given empirically by

$$\frac{d_n}{d_{jm}} = 0.485 \left[ \frac{d_n}{\left( \frac{\sigma}{g\Delta\rho} \right)^{0.5}} \right]^2 + 1; \quad \frac{d_n}{\left( \frac{\sigma}{g\Delta\rho} \right)^{0.5}} < 0.785 \tag{3}$$

$$\frac{d_n}{d_{jm}} = \frac{1.51\,d_n}{\left( \frac{\sigma}{g\Delta\rho} \right)^{0.5}} + 0.12; \quad \frac{d_n}{\left( \frac{\sigma}{g\Delta\rho} \right)^{0.5}} > 0.785 \tag{4}$$

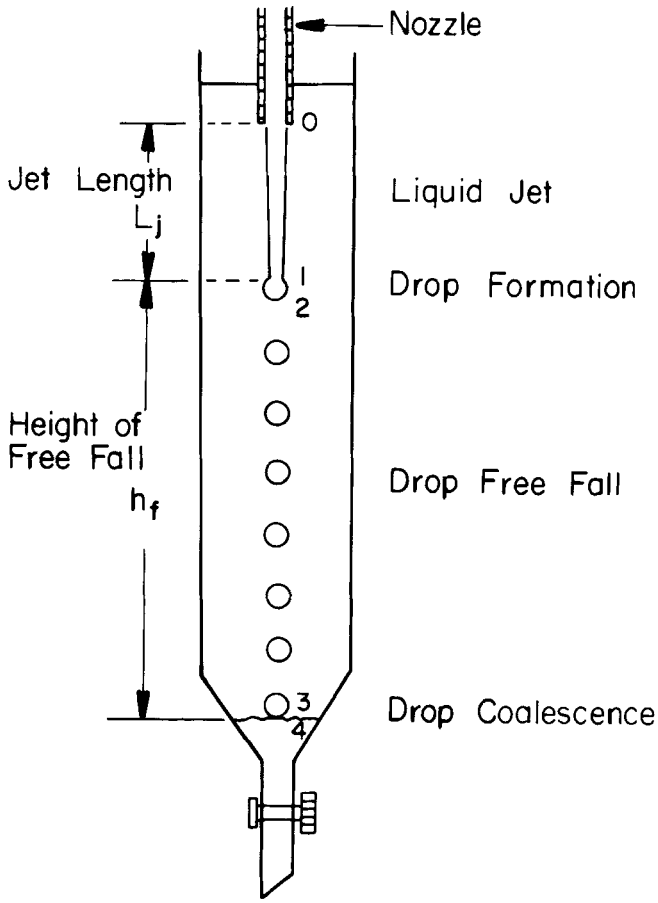


**Fig. 1. Simulated stage of a perforated plate column with a single jet nozzle.**

Skelland and Johnson (1974) measured the major and minor axes of projected drop images and obtained a drop size correlation which passes through a minimum near the predicted value of $U_{nm}$ for six Newtonian liquid-liquid systems in the absence of mass transfer.

#### Mass Transfer from (or to) a Liquid Jet

Mass transfer from (or to) a laminar jet has been used by many researchers for diffusion studies. According to Sherwood et al. (1975), numerous workers employing laminar liquid jets have checked the penetration theory quite closely without requiring any allowance for a surface effect both in gas absorption and in transfer between the jet and a surrounding liquid.

In their studies of the effect of mass transfer on liquid jet breakup, Burkholder and Berg (1974) also suggested that the experimental situation is best described as penetration-type mass transfer between a cylinder of initial concentration $(C_{Ad})_i$ and an infinite medium of initial concentration $(C_{Ac})_i$. The jet lifetimes $(t = L_j/U_j)$ for typical experiments are short, so that the boundary-layer thickness $(\delta_m \approx \sqrt{Dt})$ is small relative to the jet radius and the solute concentration profiles in both phases are strongly nonlinear. The jet itself may therefore be considered a semiinfinite medium.

#### Mass Transfer During Drop Formation, Free Fall, and Coalescence

Reviews of mass transfer during drop formation, free fall (or rise), and coalescence have been given by Skelland (1974) and Minhas (1969). From this collection, Skelland and Conger (1973) used the following in their design procedure for nonjetting conditions.

1. During drop formation [Skelland and Minhas (1971)]:

$$k^*_{df} = 0.0432\left(\frac{d_D}{t_f}\right)\left(\frac{U_n^2}{d_D g}\right)^{0.089}\left(\frac{d_D^2}{t_f D_d}\right)^{-0.334}\left(\frac{\mu_d}{\sqrt{\rho_d d_D \sigma}}\right)^{-0.601} \quad (5)$$

2. During drop free fall:
stagnant drops [Vermeulen (1953) and Johnson et al. (1958)]:

$$k^*_{dr} = -\frac{d_D}{6t}\ln\left[1 - \frac{\pi D_d^{1/2} t^{1/2}}{d_D/2}\right] \quad \text{when} \quad E_f < 0.5 \quad (6)$$

circulating drops [Skelland and Wellek (1964)]:

$$k^*_{dr} = 31.4\frac{D_d}{d_D}\left(\frac{4D_d t}{d_D^2}\right)^{-0.34}\left(\frac{\mu_d}{\rho_d D_d}\right)^{-0.125}\left(\frac{d_D U_s^2 \rho_c}{\sigma}\right)^{0.37} \quad (7)$$

oscillating drops [Skelland and Wellek (1964)]:

$$k^*_{dr} = 0.32\frac{D_d}{d_D}\left(\frac{4D_d t}{d_D^2}\right)^{-0.14}\left(\frac{d_D U_s \rho_c}{\mu_c}\right)^{0.68}\left(\frac{\sigma^3 \rho_c^2}{g\mu_c^4 \Delta\rho}\right)^{0.10} \quad (8)$$

3. During drop coalescence beneath the plate above [Skelland and Minhas (1971)]:

$$k^*_{dc} = 0.173\left(\frac{d_D}{t_f}\right)\left(\frac{\mu_d}{\rho_d D_d}\right)^{-1.115}\left(\frac{\Delta\rho\, g\, d_D^2}{\sigma}\right)^{1.302}\left(\frac{U_s^2 t_f}{D_d}\right)^{0.146} \quad (9)$$

### MASS TRANSFER THEORY

Consider a simulated stage of a perforated plate column with a single jet nozzle as shown in Figure 1. The following assumptions will be made:

1. Equilibrium solute concentrations prevail at the interface.
2. Resistance to mass transfer in the continuous phase is negligible, so that the continuous phase solute concentration at the interface is the same as the bulk concentration.
3. The dispersed phase solute concentration at the interface changes very little over the duration of a run, so that its arithmetic average at the start and the end of a run can be used.
4. The log mean concentration difference can be approximated by the arithmetic mean value.

For mass transfer into the continuous phase, and with $C_{Ac}$ uniform for a given stage because of the mixing provided by the moving drops, the total rate of dispersed phase controlled mass transfer is the sum of that occurring from the jet, during drop formation, during free fall, and during coalescence, or

$$q = k_{dj}A_j(\Delta C_{Aj})_{av} + k_{df}A_f(\Delta C_{Af})_{av} + k_{dr}A_r(\Delta C_{Ar})_{av} + k_{dc}A_c(\Delta C_{Ac})_{av} \quad (10)$$

If the average solute concentration in the continuous phase is $C_{Ac}^*$, then the dispersed phase solute concentration at the interface will be at the equilibrium concentration $C_{Ad}^*$. The following development is a considerable modification of that presented by Minhas (1969). From

$$(\Delta C_{Aj})_{av} = \frac{1}{2}(C_{Ad0} + C_{Ad1}) - C_{Ad}^*$$

$$C_{Ad1} = 2[(\Delta C_{Aj})_{av} + C_{Ad}^*] - C_{Ad0} \quad (11)$$

From

$$k_{dj}A_j(\Delta C_{Aj})_{av} = Q(C_{Ad0} - C_{Ad1})$$

$$C_{Ad1} = C_{Ad0} - \frac{k_{dj}A_j}{Q}(\Delta C_{Aj})_{av} = C_{Ad0} - T_j(\Delta C_{Aj})_{av} \quad (12)$$

From Equations (11) and (12)

$$(\Delta C_{Aj})_{av} = \frac{2(C_{Ad0} - C_{Ad}^*)}{2 + T_j} = \frac{2(\Delta C_A)}{2 + T_j} \quad (13)$$

Continuation of this treatment into the drop formation, free fall, and coalescence periods leads to the following expressions for $(\Delta C_{Af})_{av}$, $(\Delta C_{Ar})_{av}$, and $(\Delta C_{Ac})_{av}$, as developed elsewhere (Huang, 1976):

$$(\Delta C_{Af})_{av} = \frac{2(\Delta C_A)(2 - T_j)}{(2 + T_j)(2 + T_f)} \quad (14)$$

$$(\Delta C_{Ar})_{av} = \frac{2(\Delta C_A)(2 - T_j)(2 - T_f)}{(2 + T_j)(2 + T_f)(2 + T_r)} \quad (15)$$

$$(\Delta C_{Ac})_{av} = \frac{2(\Delta C_A)(2 - T_j)(2 - T_f)(2 - T_r)}{(2 + T_j)(2 + T_f)(2 + T_r)(2 + T_c)} \quad (16)$$

$$q = \frac{2(\Delta C_A)}{2 + T_j}\left[k_{dj}A_j + k_{df}A_f\frac{(2 - T_j)}{(2 + T_f)} + k_{dr}A_r\frac{(2 - T_j)(2 - T_f)}{(2 + T_f)(2 + T_r)} + k_{dc}A_c\frac{(2 - T_j)(2 - T_f)(2 - T_r)}{(2 + T_f)(2 + T_r)(2 + T_c)}\right] \quad (17)$$

where

$$T_j = \frac{k_{dj}A_j}{Q}, \quad T_f = \frac{k_{df}A_f}{Q}, \quad T_r = \frac{k_{dr}A_r}{Q}, \quad T_c = \frac{k_{dc}A_c}{Q}, \quad \text{and} \quad (\Delta C_A) = C_{Ad0} - C_{Ad}^*$$

In order to predict the rate of mass transfer, one needs the values of $k_{dj}$, $k_{df}$, $k_{dr}$, and $k_{dc}$, as well as the area for mass transfer in every stage. The evaluation of $k_{df}$, $k_{dr}$, and $k_{dc}$ has been the subject of study by many researchers. The assumption will be made here that transfer during the formation of drops at the end of a jet is the same as at a nozzle tip. We therefore assume that Skelland and Minhas' (1971) correlations for the mass transfer coefficients during drop formation [Equation (5)] and coalescence [Equation (9)] can be applied to the present work. The coefficients of mass transfer during drop free fall will be chosen according to the drop behavior, that is, whether the drops are stagnant [Equation (6)], circulating [Equation (7)], or oscillating [Equation (8)] as they fall through the extraction column.

If the coalescence interface is kept at the narrow exit of the extraction column, the mass transfer during drop coalescence can be neglected as suggested by Minhas (1969) and by Lindland and Terjesen (1956).

Several theoretical models will be considered here for the evaluation of $k_{dj}$, and their validity can be checked by comparing the theoretical predictions with the experimental results.

### The Penetration Theory

Because of the drop movement in the extraction column, the continuous phase solute concentration is assumed to be homogeneous and constant at the arithmetic average value of the initial and final solute concentrations in the continuous phase during the run. The thickness of the concentration boundary layer inside the jet is very small compared to the jet radius, and the jet itself can be considered as a semiinfinite medium. With the further assumption of uniform plug flow in the jet, the average mass transfer coefficient can be obtained as

$$k_{dj} = (k^*)_{av} = 2\left(\frac{D_d}{\pi t_e}\right)^{1/2}; \quad t_e = L_j/U_j \quad (18)$$

### Graetz-Type Solutions

Even though numerous workers have shown the success of the penetration theory for jets, it is natural to think that the prediction of mass transfer may be improved if one considers the velocity distribution inside the jet stream and solves the mass transfer problem with a Graetz type of solution.

The velocity distribution in the jet will be somewhere between a uniform plug and parabolic if the velocity distribution at the exit from the nozzle is parabolic. The longer the jet the closer the velocity distribution approaches uniform plug flow. It would be impractical to solve the flow and mass transfer problems together numerically because of the complexity of the jet breakup. Therefore, simple velocity distributions will be assumed, and the results will be compared with the experimental values to show the success of this approach.

Since the resistance to mass transfer lies mostly inside the jet in the present work, the solute concentration in the continuous phase can be considered as homogeneous with concentration $(C_{Aci} + C_{Acf})/2$. Then, the dispersed phase concentration at the jet surface can be regarded as constant at $C_{Ad}^*$. The solute concentration in the dispersed phase does not vary greatly from the nozzle tip to the end of the jet. Thus the log mean concentration driving force in the jet can be approximated by the arithmetic mean value. The mass transfer problem can be visualized as in-

Table 1. Physical and Transport Properties

| System | $\sigma$ (dyne/cm) | $\rho_d$ (g/ml) | $\rho_c$ (g/ml) | $\mu_d$ (g/cm-s) | $\mu_c$ (g/cm-s) | $D_d$ (cm²/s) | $D_c$ (cm²/s) | Temperature** (°C) |
|---|---|---|---|---|---|---|---|---|
| 1 | 24.28 | 1.106 | 0.9976 | $7.55 \times 10^{-3}$ | $1.0 \times 10^{-2}$ | $2.072 \times 10^{-5}$* | $1.24 \times 10^{-5}$* | 23.5 |
| 2 | 24.88 | 1.2425 | 0.9971 | $3.70 \times 10^{-2}$ | $9.1 \times 10^{-3}$ | $6.9511 \times 10^{-6}$* | $1.24 \times 10^{-5}$* | 25 |
| 3 | 30.0 | 1.569 | 0.9971 | $5.70 \times 10^{-3}$ | $9.1 \times 10^{-3}$ | $1.49 \times 10^{-5}$† | $1.24 \times 10^{-5}$* | 25 |
| 4 | 4.94 | 0.9981 | 0.813 | $1.01 \times 10^{-2}$ | $3.9 \times 10^{-2}$ | $1.2116 \times 10^{-5}$ | $2.66 \times 10^{-6}$ | 25 |

* Reference: Minhas (1969).
† Reference: Perry (1963).
** Run temperature.

volving flow either through an imaginary cylindrical tube with an average jet diameter of $(d_n + d_{jc})/2$ or, alternatively, through a truncated cone with diameters $d_n$ and $d_{jc}$. In either case, solute is transferred from the bulk of the disperse phase to the jet wall. Four alternative steady state flow conditions will then be assumed in turn as follows.

1. Tube plug flow (see, for example, Skelland, p. 158, 1974):

$$\frac{k_{dj}d_t}{D_d} = \frac{(k^*)_{lm}d_t}{D_d} = \frac{1}{4}\left(\frac{d_t}{L_j}\right) N_{Re}N_{Sc} \ln\left\{4\sum_{i=1}^{\infty} a_i^{-2}\exp\left[\frac{-2a_i^2(z/r_t)}{N_{Re}N_{Sc}}\right]\right\}^{-1} \quad (19)$$

2. Tube parabolic flow (Hausen, 1943):

$$\frac{k_{dj}d_t}{D_d} = \frac{(k^*)_{lm}d_t}{D_d} = 3.66 + \frac{0.0668(d_t/z)N_{Re}N_{Sc}}{1 + 0.04[(d_t/z)N_{Re}N_{Sc}]^{2/3}} \quad (20)$$

3. Cone plug flow (Cobble, 1962; Huang, 1976):

$$k_{dj} = (k^*)_{av} = \frac{2Q\left[1 - 4\sum_{i=1}^{\infty}\frac{\left(\frac{B-2r_1}{B-2r_2}\right)^{\frac{1}{2}\left(\frac{a_i}{\theta_o}\right)^2}}{a_i^2}\right]}{\pi\sin\theta_o\,(r_2^2 - r_1^2)\left[1 + 4\sum_{i=1}^{\infty}\frac{\left(\frac{B-2r_1}{B-2r_2}\right)^{\frac{1}{2}\left(\frac{a_i}{\theta_o}\right)^2}}{a_i^2}\right]} \quad (21)$$

4. Cone parabolic flow (Huang, 1976):

Assume that the difference between the mass transfer rates with plug and parabolic velocity distributions, divided by the rate with the plug distribution, is the same for both cone and tube configurations. This leads to

$$q_{\text{cone-parabolic flow}} = q_{\text{cone-plug flow}} - q_{\text{cone-plug flow}}\left[\frac{q_{\text{tube-plug flow}} - q_{\text{tube-parabolic flow}}}{q_{\text{tube-plug flow}}}\right] \quad (22)$$

## EXPERIMENTAL DETAILS

### Choice of Materials

In order to study the dispersed phase controlled mass transfer, it was necessary to use systems in which the distribution ratio greatly favored the continuous phase. The following systems were selected, in which the dispersed phase is mentioned first, followed by the solute and continuous phase, respectively.

System 1: chlorobenzene-acetic acid-water
System 2: (Nujol-carbon tetrachloride)-acetic acid-water
System 3: carbon tetrachloride-acetic acid-water
System 4: water-benzoic acid-isoamyl alcohol

Solute transfer was from the organic to the aqueous phase for systems 1 to 3 and in the reverse direction for system 4. Initial solute concentrations were roughly 2% in systems 1 to 3 and 0.1% in system 4.

Visual experiments with aluminum powder inside the drops showed stagnant, oscillating, and internally circulating behavior during drop free fall through the continuous phase for system 1, systems 2 and 3, and system 4, respectively. The dispersed phase for system 2 consisted of a 50% by volume mixture of mineral oil (Nujol) and carbon tetrachloride. Nujol was used to increase the viscosity of the dispersed phase and, according to Minhas (1969), is inert to carbon tetrachloride and acetic acid. Double distilled water was used for all experiments.

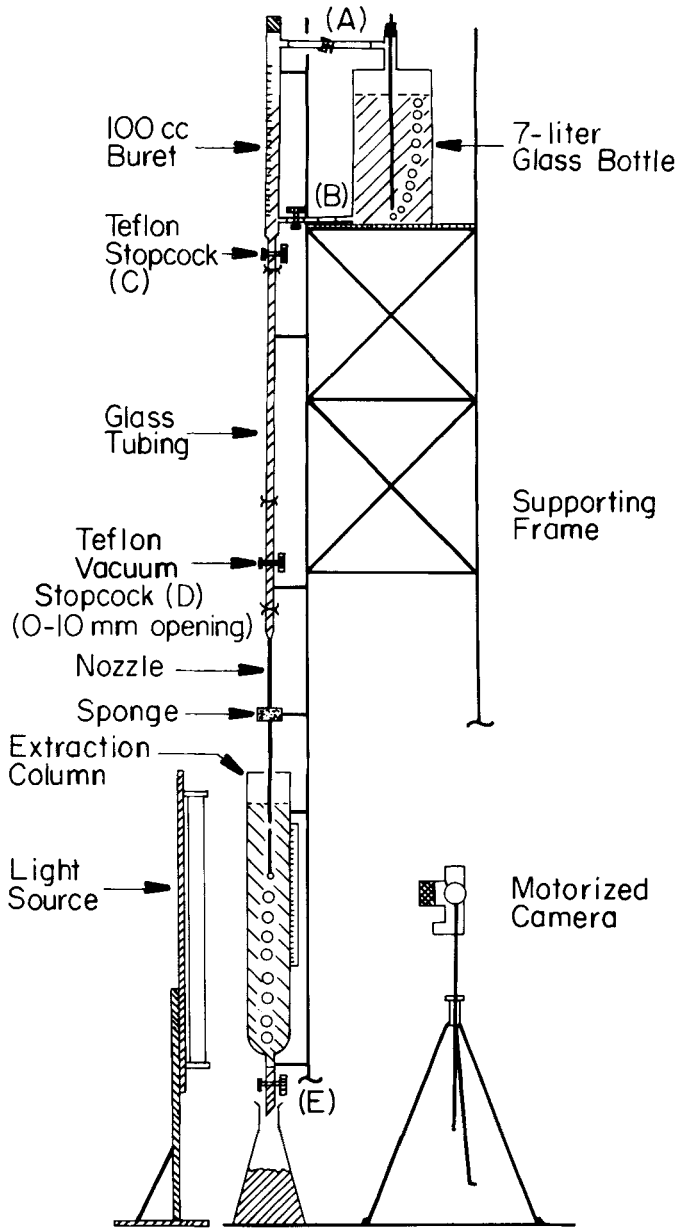


Fig. 2. Diagram of the apparatus.

### Measurement of Physical and Transport Properties

Interfacial tension was measured with a Fisher surface tensiometer, model 20, in the presence of solute at the average concentration of the experimental runs. (Bulk equilibrium was not established.) Viscosity was determined with Cannon-Fenske routine viscometers, ASTM 25 and 100; density was evaluated by weighing the liquid in known volume, and diffusivities were taken from the literature. The diffusivity of benzoic acid in isoamyl alcohol was calculated by Reddy and Doraiswamy's equation (1967):

$$\frac{D^o_{AB}\mu_B}{T} = \frac{10 \times 10^{-8} M_B^{1/2}}{V_{bA}^{1/3}V_{bB}^{1/3}}; \quad \frac{V_{bB}}{V_{bA}} \leq 1.5 \quad (23)$$

The properties thus obtained are shown in Table 1.

### Apparatus

The apparatus is shown in Figure 2. A 100 cm$^3$ buret was connected to a 7 l, narrow necked glass bottle at both

the neck and the bottom of the bottle, using Tygon and shrinkable Teflon tubing, respectively. This served as the reservoir for the dispersed phase liquid. Rubber stoppers were fitted into both the buret and the bottle as shown; a 0.15 cm I.D. capillary tube was then inserted through the rubber stopper to the bottom of the bottle. This device gave a constant flow rate for the dispersed phase. Only a few seconds were needed after start-up to establish a constant head, as revealed by air bubbles issuing from the bottom of the capillary tube. To provide enough head for jetting conditions, a 60 cm section of 0.7 cm I.D. glass tubing was attached below the buret. Following this was an additional 30 cm section having a Teflon vacuum stopcock with a 0 to 10 mm opening. A thin walled glass nozzle was attached below the control stopcock section. Each of the nozzles was 60 cm long to ensure fully developed velocity profiles, and special care was taken to make the plane of the tip and the axis of the nozzle at right angles to each other. Inner (and outer) diameters of the five nozzles used were as follows: 0.173 cm, (0.292); 0.239, (0.401); 0.325, (0.495); 0.394, (0.597); 0.503, (0.711). All attachments were made with 10/30 Pyrex glass tapered joints, fastened with rubber bands, and a sponge was used to damp out shocks that might cause the nozzle to vibrate.

Two glass columns resembling Figure 1, with 7 cm I.D. and lengths of 32 and 55 cm, served as reservoirs for the continuous phase. The 32 cm column was used as a preparatory column for the establishment of the desired flow rate and jet length. The longer column was then used for extraction purposes.

The extraction column was filled with various amounts of continuous phase to give different free fall heights, and a scale was attached to the side of the column to permit photographic measurement of jet length. For drop size and jet contraction measurements, a 5 gal aquarium with plane glass sides was used instead of the extraction column.

The extracted dispersed phase was collected at the exit from the column in an Erlenmeyer flask. To avoid contamination by foreign substances, only Pyrex glass and Teflon were used to contain the liquid in the whole system.

Two parallel 20 W fluorescent lights mounted vertically on a board, about 6 cm apart, served as the lighting system for the photographic study. This board was fastened about 20 cm behind the extraction column on a supporting frame with adjustable height.

The motorized camera (Nikon F-2 with 55 mm f/3.5 Micro-Nikkor lens and MD-2 motor drive) was mounted on a tripod. Kodak Tri-X Pan film with ASA 400 was used with a shutter speed of 1/1 000 s and aperture setting of f/3.5-f/5.6. A Gossen Luna-Pro exposure meter was used to determine the exposure setting.

#### Experimental Procedure

The solvents used as the dispersed and continuous phases were saturated with each other before the experiments were performed.

About 4 l of dispersed phase liquid were placed in the reservoir bottle, and the tip of the nozzle was then immersed in the dispersed phase liquid in a separate flask. With the clamp (A) and stopcock (B) closed, the dispersed phase liquid was drawn by a rubber suction bulb into the nozzle and tube section until the level of the liquid reached above the buret stopcock (C). The control stopcock (D) was then closed. The liquid level in the buret was the same as the level in the reservoir bottle after the clamp (A) and stopcock (B) were opened. This procedure was necessary to avoid trapping air bubbles in the flow system.

The dispersed phase flask was next replaced by the preparatory column filled with continuous phase. The vacuum stopcock (D) was slowly opened, and the liquid flow was adjusted to the desired flow rate and jet length. Steady state was established right after the start-up. The buret stopcock (C) was then closed to stop the flow. The same flow rate and jet length could be reestablished by the opening of this stopcock. The extraction column, filled with continuous phase to give the desired free fall height, was then substituted for the preparatory column. The nozzle tip was, of course, immersed in the continuous phase in all runs.

A stopwatch was started when the buret stopcock (C) was opened. For runs without drop coalescence, the coalescence level was kept constant in the narrow exit of the extraction column, so that the effect of mass transfer due to coalescence could be neglected. For runs with drop coalescence, the coalescence level was kept constant in the cone section of the extraction column by stopcock (E).

Five pictures were taken during the run, and the stopwatch and flow were then stopped by closing the buret

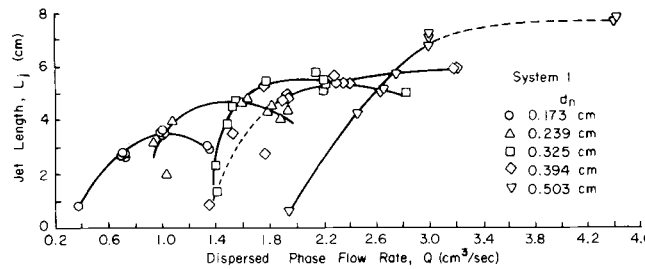


**Fig. 3. Jet length vs. dispersed phase flow rate for the high interfacial tension system 1 (chlorobenzene-acetic acid-water).**

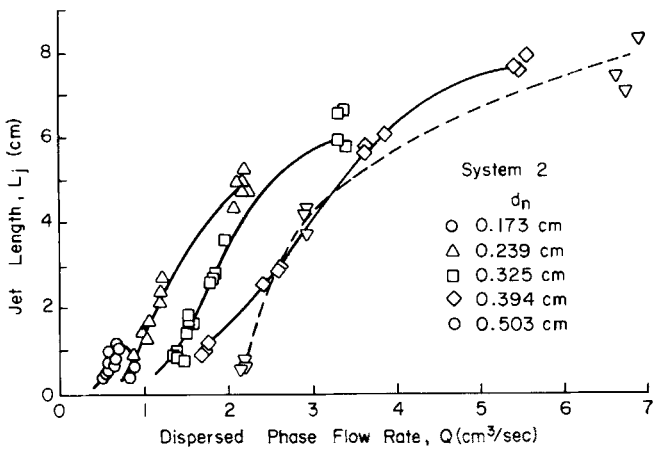


**Fig. 4. Jet length vs. dispersed phase flow rate for the high interfacial tension system 2 (Nujol-carbon tetrachloride)-acetic acid-water.**

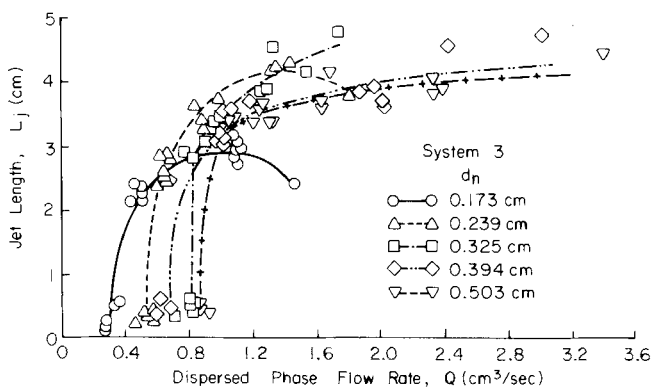


**Fig. 5. Jet length vs. dispersed phase flow rate for the high interfacial tension system 3 (carbon tetrachloride-acetic acid water).**

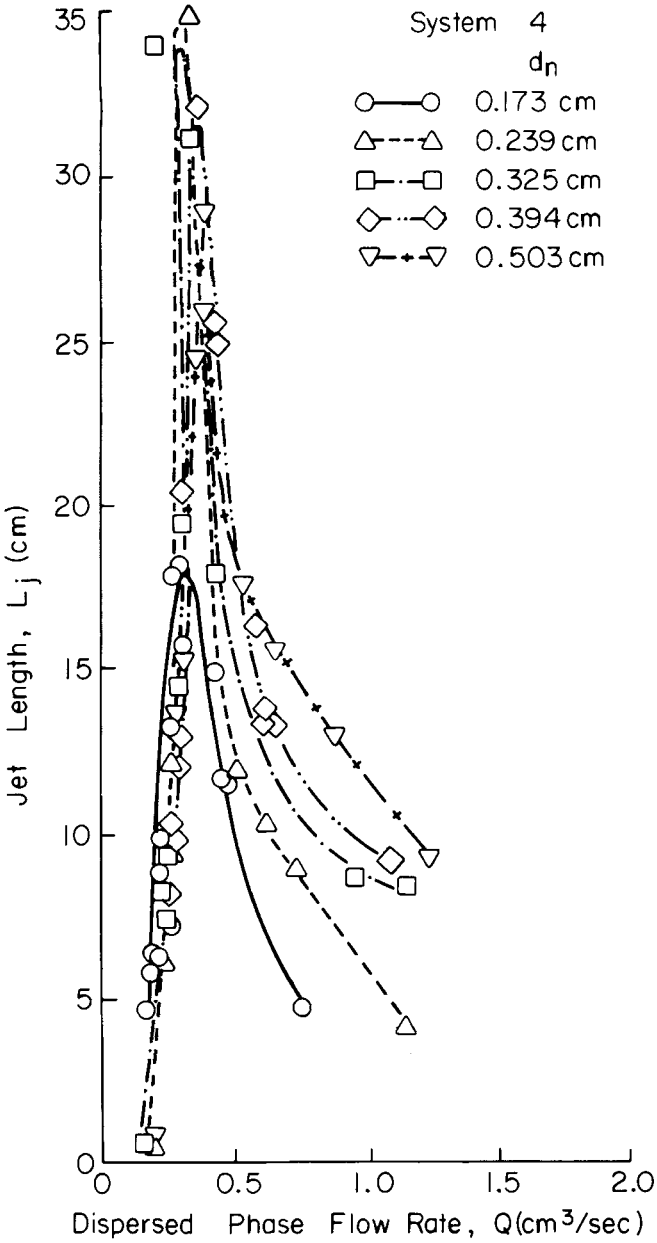


Fig. 6. Jet length vs. dispersed phase flow rate for the low interfacial tension system 4 (water-benzoic acid-isoamyl alcohol).

stopcock. Readings of the buret scale were made before and after the run to obtain the volume of the dispersed phase expelled by the nozzle. A calibration of the actual volume expelled from the nozzle vs. the buret reading resulted in a ratio of 70.5 ml per 1 ml buret reading.

Three different free fall heights were used for the same flow rate and jet length. Twelve such runs were attempted for each nozzle over the entire region of the jetting flow rates.

The volume of the continuous phase was measured at the end of the run, and the amount of solute transfer was determined by titrating the water phase against standard 0.2 N sodium hydroxide solution.

After all nozzles had been used for a particular system, the apparatus was taken apart and cleaned with $K_2Cr_2O_7$-$H_2SO_4$ cleaning solution. Every piece of the apparatus was then thoroughly rinsed with double distilled water.

The photographic film was developed, and the negatives were viewed with a microfiche reader. Jet lengths were measured directly from the projected image, and the number of drops between the jet breakup point and the coalescence level was counted. Average values of the jet length and drop count were used for each run.

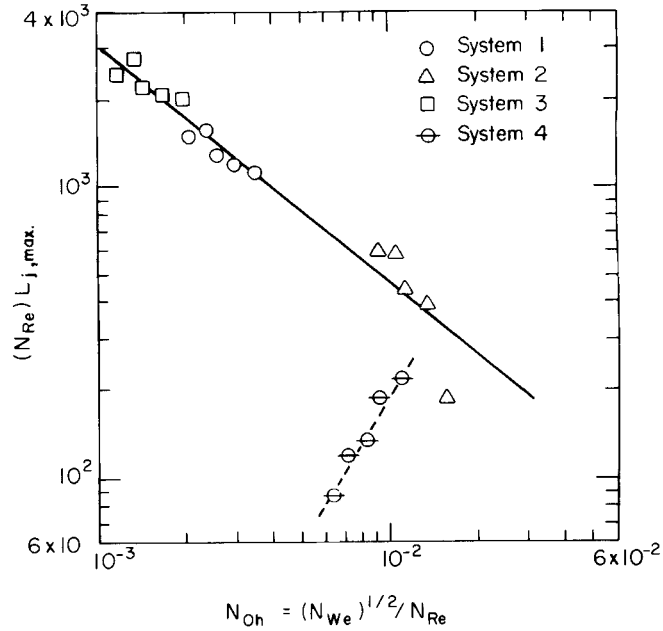


Fig. 7. Correlation of flow rate at maximum jet length. Data from all five nozzle sizes are included here.

For drop size and jet contraction measurements, separate runs were made with the aquarium replacing the extraction column. The following measurements were made for each negative: major and minor axes on all measurable drops, the outside diameter of the nozzle (for calibration purposes), and the diameter of the jet at breakup.

## DISCUSSION OF EXPERIMENTAL RESULTS

### Jet Length for Individual Systems

Plots were made of the measured jet lengths vs. dispersed phase flow rates ($L_j$ vs. $Q$) for all the data. They are shown in Figures 3 to 5 for the high interfacial tension systems and in Figure 6 for the low interfacial tension system. Because of the low interfacial tension and high continuous phase viscosity, jet lengths in system 4 are much longer than those in systems 1, 2, and 3.

Some of the $L_j$-$Q$ plots show a maximum. The velocity at this maximum, in addition to being of practical importance, describes a unique point on the $L_j$-$Q$ curve. A correlation of this velocity can be obtained by plotting $(N_{Re})_{Lj,max}$ vs. $N_{Oh}$, as suggested by Grant and Middleman (1966), and this is given in Figure 7. Evidently the data for the low interfacial tension system do not agree with those for the high interfacial tension systems.

### Generalized Jet Length Correlation

Attempts were made to obtain a generalized jet-length correlation for all four systems for flow rates up to the maximum jet length (the so-called varicose region), since this is the most suitable range of extraction operation according to Mayfield and Church (1952).

Correlations were first tried by assuming that the effect of viscosity can be neglected. One can then plot the jet-length data as $L_j/d_n$ vs. $(N_{We})^{1/2}$, following previous workers. Results are shown in Figures 8 and 9 for the high and the low interfacial tension systems, respectively. It seems that an individual correlation will be needed for each system if the jet-length data are treated in this manner.

For a more general correlation, let

$$L_j = f(d_n, U_n, \rho_d, \rho_c, \mu_d, \mu_c, \sigma) \qquad (24)$$

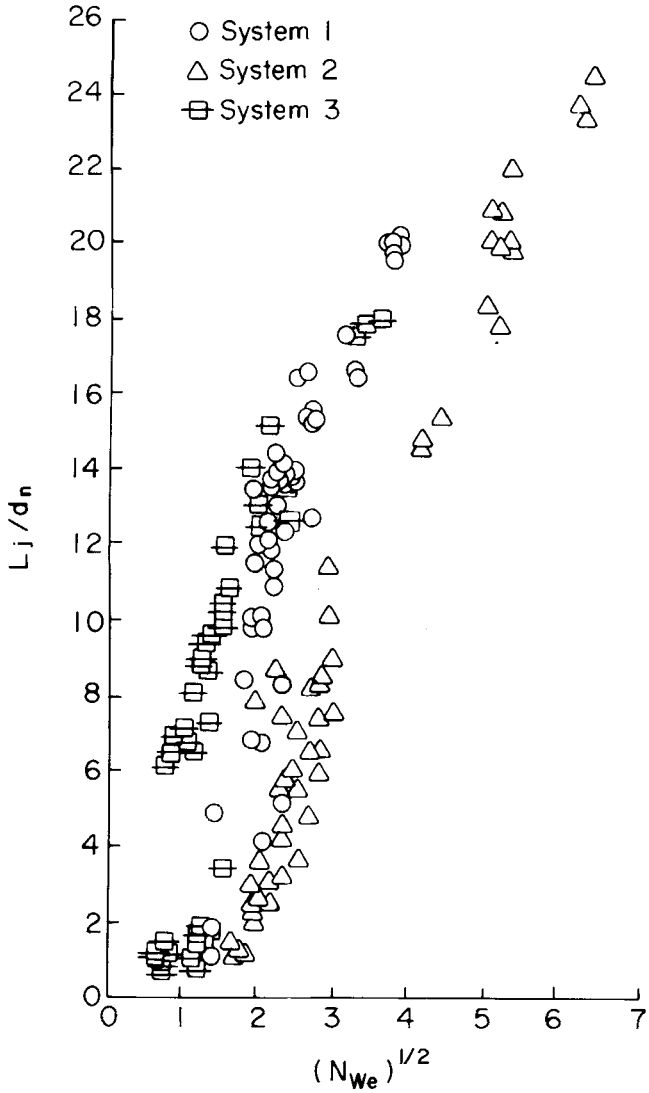


Fig. 8. Jet length correlation as $L_j/d_n$ vs. $(N_{We})^{1/2}$ for the high interfacial tension systems. Data from all five nozzle sizes are included here.

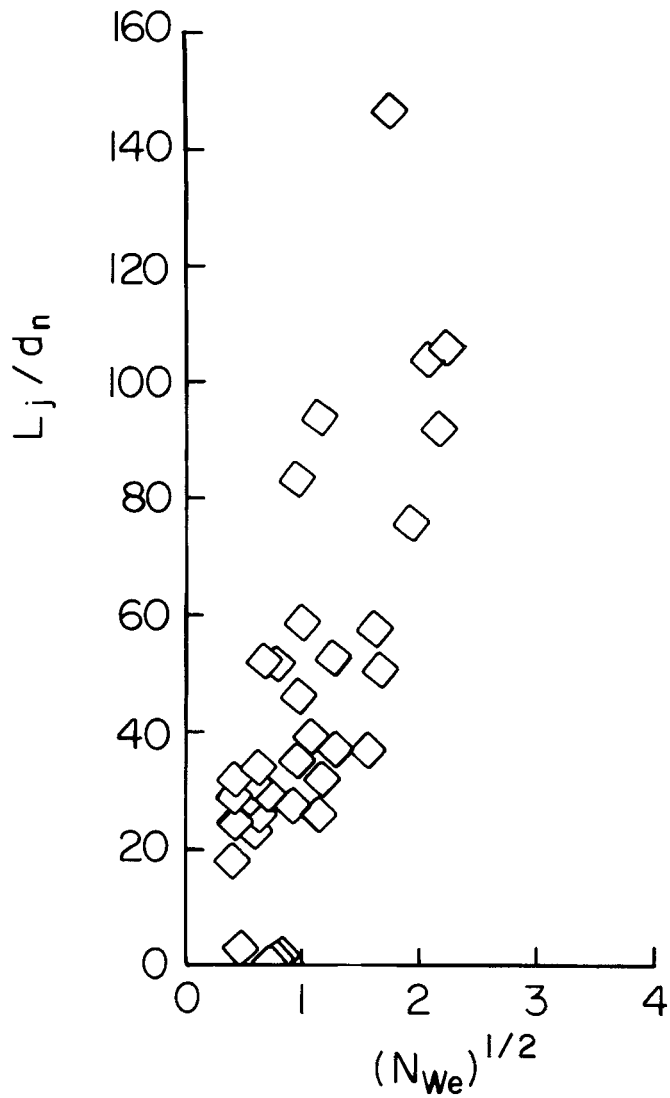


Fig. 9. Jet length correlation as $L_j/d_n$ vs. $(N_{We})^{1/2}$ for the low interfacial tension system 4. Data from all five nozzle sizes are included here.

A dimensional analysis of this expression and the assumption of an exponential form led to

$$\frac{L_j}{d_n} = \alpha_1 \left(\frac{U_n^2\, d_n\, \rho_d}{\sigma}\right)^{a_1} \left(\frac{\mu_d}{U_n\, d_n\, \rho_d}\right)^{b_1} \left(\frac{\mu_c}{U_n\, d_n\, \rho_d}\right)^{c_1} \left(\frac{\rho_c}{\rho_d}\right)^{d_1} \quad (25)$$

With Equation (25) as a guide, forty-three different combinations of dimensionless groups were considered for the correlation of data from the high interfacial tension systems. The SAS (Statistical Analysis System) REGR computer program was used to obtain the best least-squares correlations for the equations chosen.

Tyler and Watkin (1932) achieved partial correlation of the streamline portion of the jet length curve (that is, the region being correlated here) in near-linear plots of $L_j/d_n$ vs. $U_n \sqrt{d_n \rho_d/\sigma}$ from measurements on liquid-liquid systems without mass transfer. This suggested that exponents on $U_n$, $d_n$, and $\sigma$ are about 1.0, 0.5, and $-0.5$, respectively, particularly when allowance is made, as below, for the fact that $U_n$ must exceed $U_{nj}$ before a jet is formed. Now Figure 6 in the paper by Meister and Scheele (1969) indicates that for the jetting region under consideration, the exponent on $U_n$ is not greatly affected by mass transfer between the jet and the surrounding liquid. This is consistent with the stratification in Figure 8 of the present study, which also implies that an exponent of about 0.5 on $d_n$ remains adequate for a given system in the presence of mass transfer.

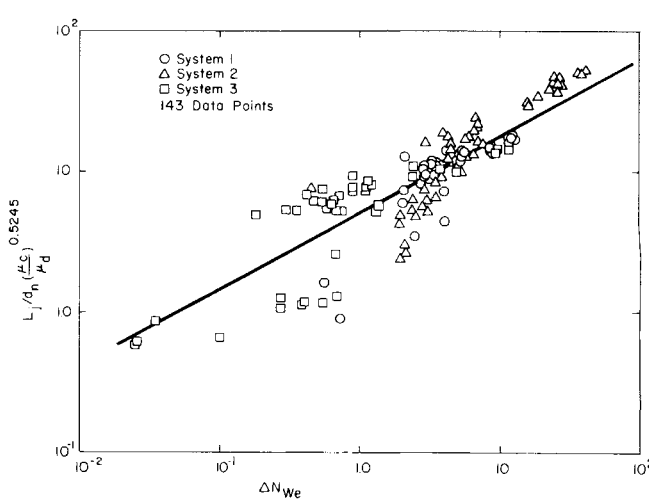


Fig. 10. Generalized jet length correlation for high interfacial tension systems. Data from all five nozzle sizes are included here.

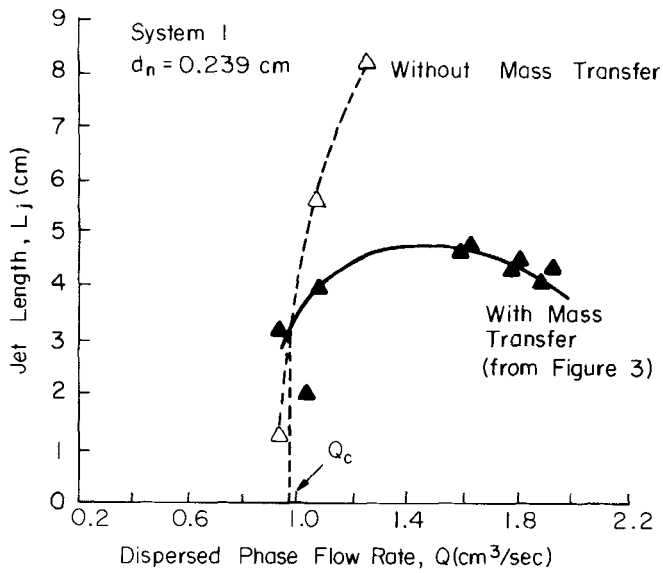


**Fig. 11. Comparison between jet lengths with and without mass transfer. (System 1 = chlorobenzene-acetic acid-water.)**

These considerations would be accommodated in Equation (25) if $a_1$ is approximately one-half and $b_1$ equals $-c_1$. However, $L_j$ is greater than zero only when $U_n$ exceeds $U_{nj}$, the jetting velocity. It may therefore be appropriate to substitute either $\Delta N_{We}$ or $\Delta N'_{We}$ for $N_{We}$ (that is, for $U_n^2\, d_n\, \rho_d/\sigma$), where $\Delta N_{We} = (U_n^2 - U_{nj}^2) d_n \rho_d/\sigma$, and $\Delta N'_{We} = (U_n - U_{nj})^2 d_n \rho_d/\sigma$, giving

$$\frac{L_j}{d_n} = \alpha\,(N_{We}, \Delta N_{We}, \text{or } \Delta N'_{We})^{1/2} \left(\frac{\mu_c}{\mu_d}\right)^{c_1} \left(\frac{\rho_c}{\rho_d}\right)^{d_1} \tag{26}$$

The final group will not be considered a variable here, since it changed only slightly in the present study (that is, $0.636 \leq \rho_c/\rho_d \leq 0.902$). Among the forty-three empirical correlations attempted, several have the form of Equation (26). In fact, Equation (27) below gives a correlation coefficient $R$ for our 143 data points of 0.830, which is close to the highest value found, namely 0.846. For more than 100 data points, $R > 0.3211$ shows correlation with better than 99.9% certainty (Fisher and Yates, 1964). (The correlations with slightly higher $R$ give substantially different exponents on $U_n$, $d_n$, and $\sigma$.) The selected correlation is therefore

$$\frac{L_j}{d_n} = 5.0767\,(\Delta N_{We})^{0.5499} \left(\frac{\mu_c}{\mu_d}\right)^{0.5245} \tag{27}$$

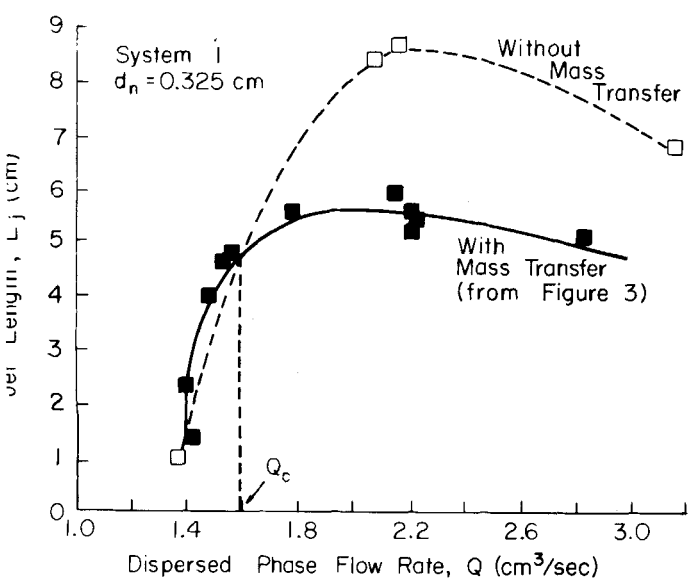


**Fig. 12. Comparison between jet lengths with and without mass transfer. (System 1 = chlorobenzene-acetic acid-water.)**

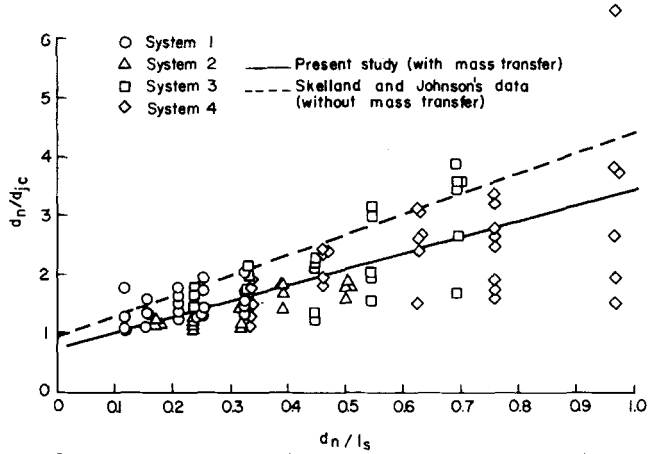


**Fig. 13. Jet contraction correlation. Data from all five nozzle sizes are included here.**

Figure 6 shows that in contrast to systems 1 to 3, $L_j$ is virtually independent of $d_n$ in the range being correlated for the low interfacial tension data of system 4. Reasons for this are unknown, but further anomalous indications for this system appear in Figure 7. It follows that Equation (27) cannot be extended to include system 4.

A plot of Equation (27) appears in Figure 10. The average absolute deviation between experimental values and those predicted from this correlation is 39.69%. Logarithmic coordinates are used in Figure 10 so as to reveal the regions of greater error. As expected, the error in correlation tends to increase with decreasing jet length, because fluctuations associated with drop formation and detachment occupy a larger fraction of the jet as its length is reduced. Additional deviations probably arise from the increased oscillation in jet length with decrease in flow velocity below $U_{nm}$, as reported by Christiansen and Hixson (16).

The directional effect of dispersed phase viscosity is the same as that observed by some previous workers for liquid jets into air (Tyler and Watkin, 1932) but is the reverse of that found by others (Grant and Middleman, 1966). According to Burkholder and Berg (1974), however, for systems undergoing mass transfer the directional effects of viscosities, densities, and solute diffusivities on the length of a liquid jet in another immiscible liquid can be reversed depending on the system and experimental conditions. The correlation obtained may therefore hold only for the range of conditions prevailing in the present study.

To consider the effect of mass transfer on jet length, experimental runs were made with pure chlorobenzene and water. The results are shown in Figures 11 and 12 for two nozzles in system 1. The jet with mass transfer to the continuous phase is shorter than the one without mass transfer at the same dispersed phase flow rate for $Q > Q_c$ in the range investigated. For $Q < Q_c$, the trend is unclear. Evidently the effect of mass transfer on jet length is complicated and depends on the system and dispersed phase flow rate.

### Jet Contraction

A plot of $d_n/d_{jc}$ vs. $d_n/l_s$ was made in Figure 13 for all runs, following Christiansen and Hixson (1957) and Skelland and Johnson (1974). A least-squares line for all the data was obtained as

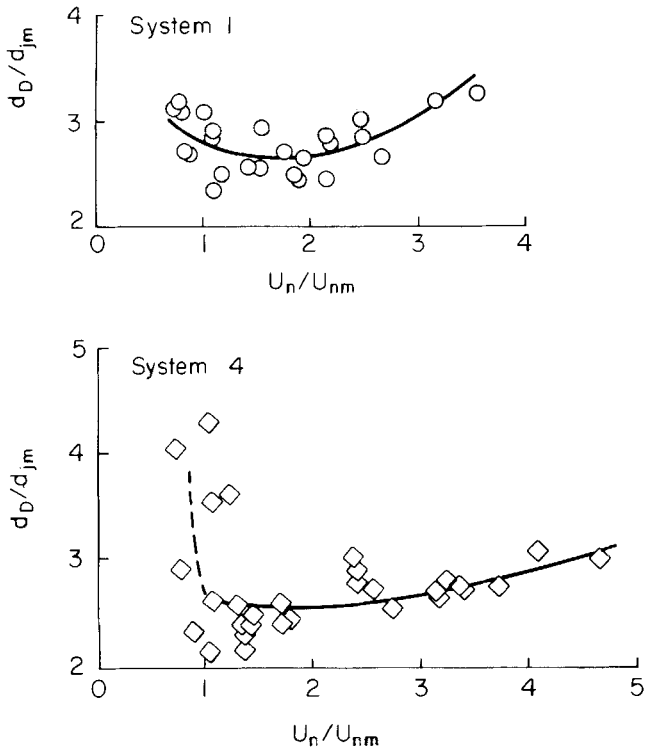


Fig. 14. Drop size correlation for systems 1 and 4. (System 1 = chlorobenzene-acetic acid-water; system 4 = water-benzoic acid-isoamyl alcohol.) Data from all five nozzle sizes are included here.

$$d_n/d_{jc} = 2.7350\ (d_n/l_s) + 0.5718 \qquad (28)$$

where $l_s = \pi(\sigma/\Delta\rho g)^{1/2}$. The average absolute deviation was 20.28%. The plot for jet contraction without mass transfer from Skelland and Johnson (1974) is also shown as a broken line in Figure 13 for comparison. It appears that mass transfer may have a moderate effect on jet contraction.

The scatter of the data at a given $d_n/l_s$ shows that the jet radius at breakup oscillated about a mean value during drop formation and detachment. It follows that only average values of jet contraction can be obtained from the above correlation.

### Drop Size from Jet Breakup

The results of drop size measurements were plotted as $d_D/d_{jm}$ vs. $U_n/U_{nm}$ as suggested by Skelland and Johnson (1974). They are shown in Figures 14 and 15 for each individual system and each nozzle size. The terms $d_{jm}$ and $U_{nm}$ were calculated from Equations (2) to (4).

The drop size correlations for systems 1 and 4 seem to be general for all nozzle sizes, whereas the drop sizes for systems 2 and 3 seem strictly to require a different correlation for each nozzle. Free fall drops in systems 2 and 3 showed oscillating behavior, but the reason for the separation of correlations for different nozzles remains unknown.

Least-squares lines were obtained for systems 1 and 4 as general equations for each system. For systems 2 and 3 together, separate least-squares lines were obtained for each nozzle size (see Huang, 1976).

For a more general relationship, all data for the different systems and nozzles were plotted in Figure 16, and a single least-squares correlation was obtained, with an average absolute deviation of 13.10%, as

$$\frac{d_D}{d_{jm}} = 3.0704 - 0.1701\left(\frac{U_n}{U_{nm}}\right) + 0.0487\left(\frac{U_n}{U_{nm}}\right)^2 \qquad (29)$$

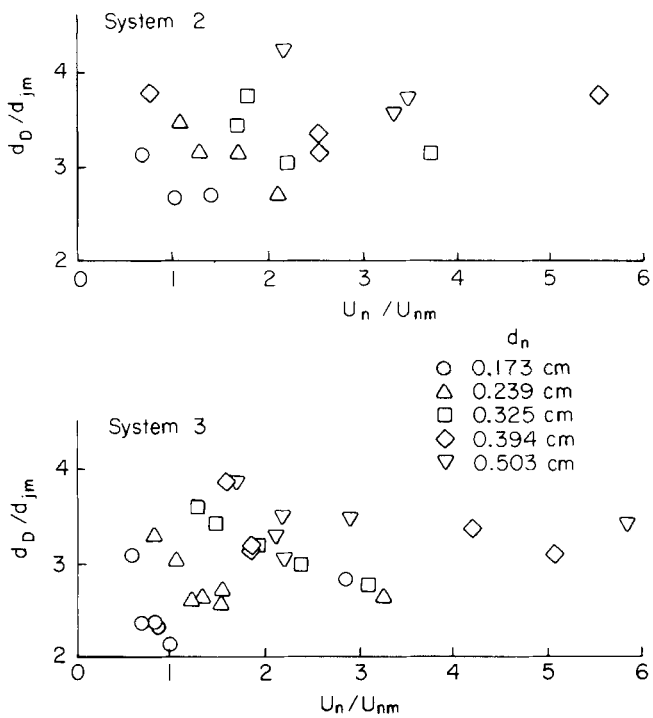


Fig. 15. Drop size correlation for systems 2 and 3. [System 2 = (Nujol-carbon tetrachloride)-acetic acid-water; system 3 = carbon tetrachloride-acetic acid-water.]

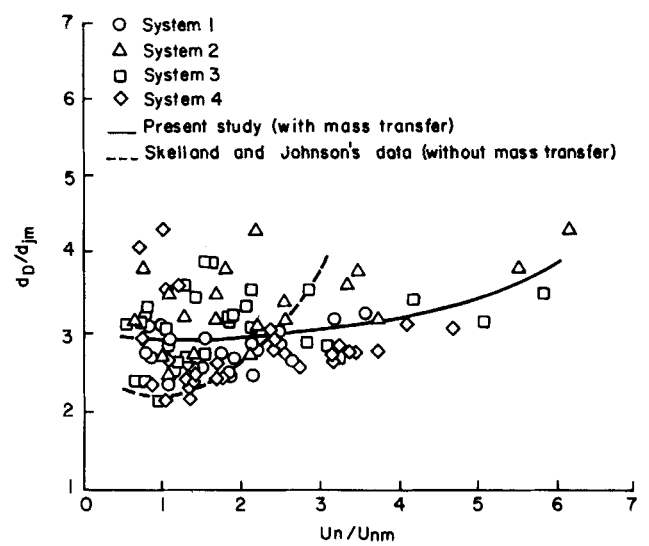


Fig. 16. Generalized drop size correlation. Data from all five nozzle sizes are included here.

The span of the data points in Figure 16 is somewhat wider than in the non-mass-transferring experiments of Skelland and Johnson (1974). The least-squares line of their data is also shown in Figure 16.

### Comparison between Predicted and Experimental Mass Transfer Rates

Photographs taken during each run gave information on jet length, drop free fall height, number of free fall drops, and location of the coalescence plane. A typical picture is shown in Figure 17 for system 3. Other photographs of parallel experiments were taken through the plane glass of the aquarium for drop size and jet contraction measurements.

After the above correlations for jet length, jet contraction, and drop size from jet breakup were obtained, a computational procedure is possible for the evaluation of areas

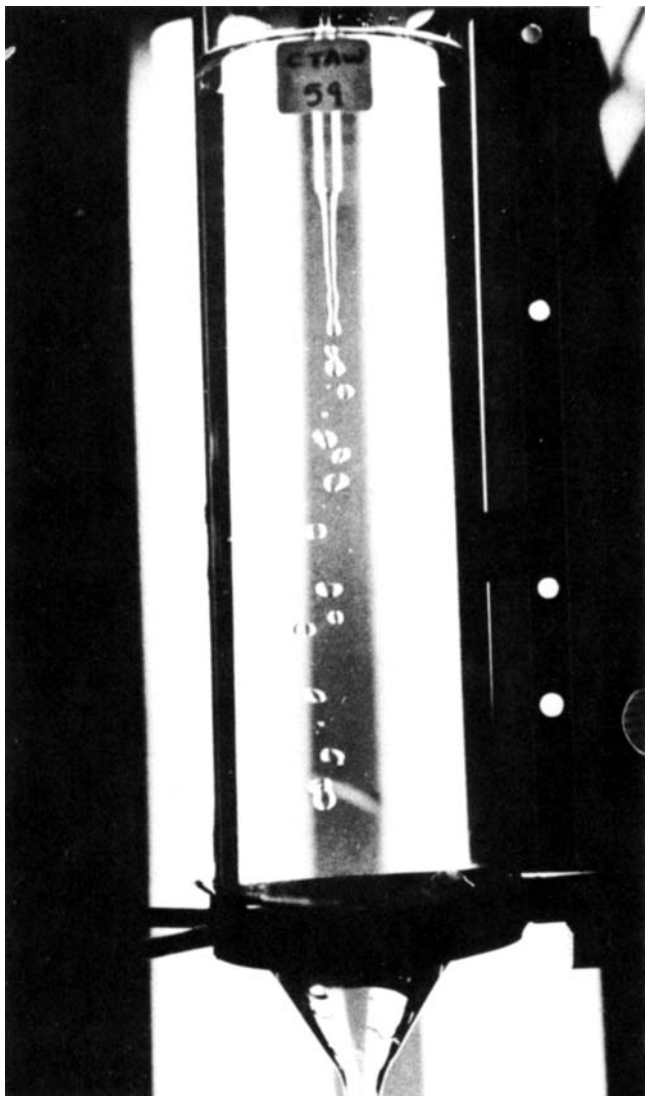

Fig. 17. Photograph of an experimental run on system 3 (carbon tetrachloride-acetic acid-water).

for mass transfer and for the prediction of mass transfer rate.

*Prediction of Mass Transfer Rate from Experimental Data.* Areas for mass transfer were calculated from the experimentally measured jet length for each run, the jet contraction from the experimental correlation [Equation (28)], and the separate drop size correlation for each system or each nozzle. Thus

$$A_{j,\text{tube}} \doteq A_{j,\text{cone}} = \pi \left( \frac{d_n + d_{jc}}{2} \right) L_j \qquad (30)$$

Table 2. Overall Average Absolute Deviation Between Experimental Mass Transfer Rates and Those Predicted Using Individual Measured Jet Lengths, Correlated Jet Contraction from Equation (28), and Separate Drop Size Correlations for Each System or Each Nozzle

| | High interfacial tension systems | All systems |
|---|---|---|
| Tube plug flow | 19.67% | 21.46% |
| Tube parabolic flow | 17.89% | 19.24% |
| Cone plug flow | 18.20% | 19.18% |
| Cone parabolic flow | 17.09% | 17.81% |
| Penetration theory | 17.41% | 18.41% |

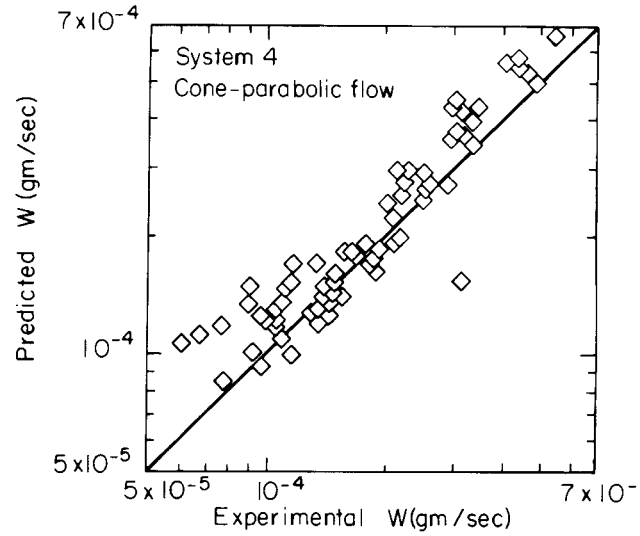


Fig. 18. Predicted vs. experimental mass transfer rates from experimental data for system 4. (System 4 = water-benzoic acid-isoamyl alcohol.) Data from all five nozzle sizes are included here.

Skelland and Minhas' correlation for mass transfer coefficients during drop formation (1971) was based on the area of the drop at detachment, so that

$$A_f = A_D = \pi d_D^2 \qquad (31)$$

At steady state, the formation of each drop coincides with the disappearance of another drop through coalescence at the plane interface. This was verified by the constancy of the number of free fall drops in the extraction column. Therefore

$$A_r = (N_D)_{\text{av}} A_D \qquad (32)$$

where $(N_D)_{\text{av}}$ represents the average number of free fall drops in the extraction column at any instant during a run.

For mass transfer during coalescence

$$A_c = \pi d_c^2/4 \qquad (33)$$

where $d_c$ is the diameter of the conical section of the extraction column where drop coalescence occurs.

Then, from Equation (17), for mass transfer with the coalescence level in the narrow exit of the extraction column (that is, systems 1, 2, and 3)

$$q = \frac{2(\Delta C_A)}{2 + T_j} \left[ k_{dj} A_j + \frac{k_{df} A_f (2 - T_j)}{(2 + T_f)} + \frac{k_{dr} A_r (2 - T_j)(2 - T_f)}{(2 + T_f)(2 + T_r)} \right] \qquad (34)$$

and

$$W = q \text{ (molecular weight of transferring solute)} \qquad (35)$$

Coalescence of the drops occurred less readily in system 4, and it was therefore convenient to allow the coalescence plane to occupy the entire cross section just above the cone. In this case $q$ is given by the unabbreviated form of Equation (17) and $W$ by Equation (35).

Predicted and experimental values of $W$ were compared for all four systems using the five different models of the jet condition represented by Equations (18) to (22). A typical graphical representation for system 4, assuming cone parabolic flow in the jet, appears in Figure 18. The full results are given in Table 2 and show that the assumption of cone parabolic flow in the jet gave the best overall prediction. It is notable that results given by the simpler penetration theory are a close second in effective-

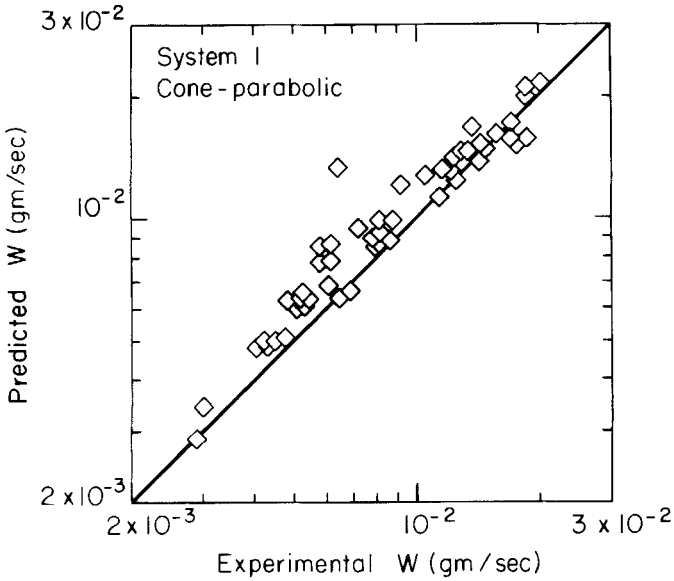


Fig. 19. Predicted vs. experimental mass transfer rates from generalized correlations for system 1. (System 1 = chlorobenzene-acetic acid-water.) Data from all five nozzle sizes are included here.

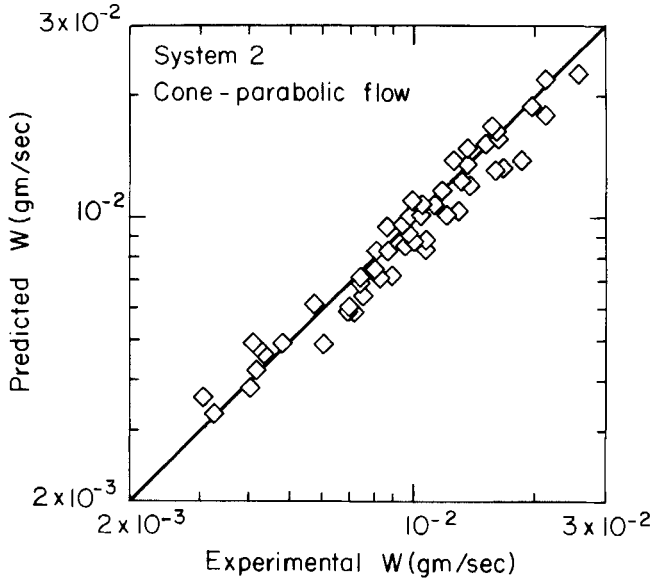


Fig. 20. Predicted vs. experimental mass transfer rates from generalized correlations for system 2. [System 2 = (Nujol-carbon tetrachloride)-acetic acid-water.] Data from all five nozzle sizes are included here.

ness. Predictions for nonoscillating and for oscillating drops were slightly higher and lower, respectively, than the experimental values.

*Prediction of Mass Transfer Rate from Generalized Correlations.* Although Table 2 shows successful prediction of mass transfer rates, $W$, when individual measurements and correlations are used for $L_j$ and $d_D$ in each run, it is perhaps of greater interest to test the effectiveness of the generalized correlations developed here for these quantities.

The predictive mass transfer computations were accordingly repeated with the following modifications.

The generalized jet length correlation for high interfacial tension systems in Equation (27) was used to predict jet lengths at experimental conditions for systems 1, 2, and 3. These predicted lengths were used to replace the experimentally measured jet length for each run in the predictions of mass transfer rates in the previous section. Drop size was obtained from the generalized drop size correlation for all systems in Equation (29). Jet contractions from Equation (28), the number of free fall drops, and the area for mass transfer during coalescence remained the same as in the previous section.

Results are presented in Figures 19 to 21 for the varicose region, assuming cone parabolic flow in the jet. All five nozzle sizes are represented in each figure. Average absolute deviations are given in Table 3 for the three combined high interfacial tension systems. The assumption of

Table 3. Overall Average Absolute Deviation between Experimental Mass Transfer Rates and Those Predicted Using The Generalized Correlations for Jet Length, Jet Contraction, and Drop Size from Equations (27), (28), and (29), Respectively

| | High interfacial tension systems |
|---|---|
| Tube plug flow | 19.26% |
| Tube parabolic flow | 17.33% |
| Cone plug flow | 17.75% |
| Cone parabolic flow | 16.35% |
| Penetration theory | 16.77% |

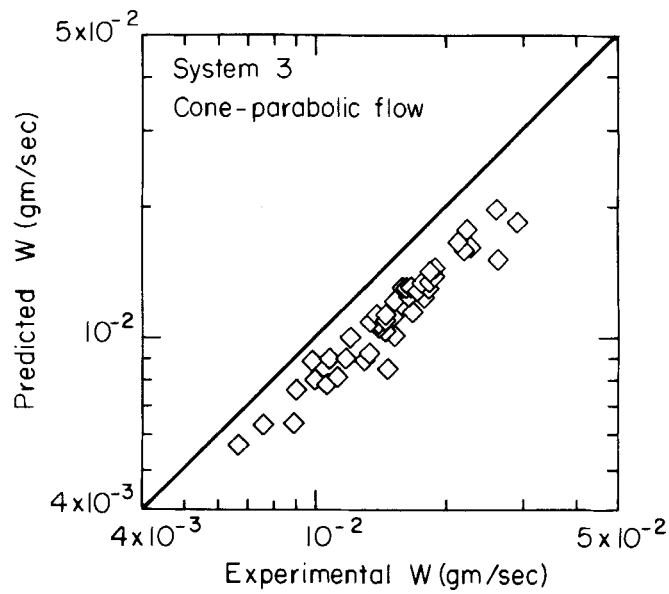


Fig. 21. Predicted vs. experimental mass transfer rates from generalized correlations for system 3. (System 3 = carbon tetrachloride-acetic acid-water.) Data from all five nozzle sizes are included here.

cone parabolic flow in the jet again gave the best overall results, with predictions from the penetration theory a close second in order of effectiveness. Once again, predictions are slightly high for the stagnant, nonoscillating drops of Figure 19 and somewhat low for the oscillating drops of Figure 21.

In the latter case it is likely that the oscillations induced in the low viscosity drops of system 3 by the violent process of jet breakup were considerably more vigorous than in the nonjetting experiments which led to Equation (8). Use of the latter equation to predict $k_{dr}$ for oscillating drops in Equation (34) may therefore account for this small discrepancy.


## ACKNOWLEDGMENT

This work was partially supported by National Science Foundation Grant No. ENG 74-17286.

## NOTATION

$A_c$ = interfacial area during drop coalescence, cm$^2$
$A_D$ = surface area of a single drop, cm$^2$
$A_f$ = interfacial area during drop formation, cm$^2$
$a_i$ = $i^{th}$ root of equation $J_0(a) = 0$
$A_j$ = interfacial area between the jet and the continuous phase, cm$^2$
$A_r$ = surface area of all free fall drops at any instant, cm$^2$
$a_1$ = constant in jet length correlations
$B$ = constant, defined by $Q/2\pi(1 - \cos\theta_o)D_d$
$b_1$ = constant in jet length correlations
$C_A$ = solute concentration, g-mole/ml
$C_{Ac}^*$, $C_{Ad}^*$ = equilibrium solute concentrations in continuous phase and dispersed phase, respectively, g-mole/ml
$(C_{Ad})_i$, $(C_{Ac})_i$ = initial concentrations of solute in dispersed and continuous phases, g-mole/ml
$(C_{Ac})_f$ = final concentration of solute in continuous phase, g-mole/ml
$C_{Ad1}$ = solute concentration in dispersed phase at location 1, g-mole/ml
$(\Delta C_A)$ = concentration driving force, defined by $C_{Ad0} - C_{Ad}^*$, g-mole/ml
$(\Delta C_{Aj})_{av}$, $(\Delta C_{Af})_{av}$, $(\Delta C_{Ar})_{av}$, $(\Delta C_{Ac})_{av}$ = arithmetic mean solute concentration driving forces during jetting, drop formation, free fall, and coalescence of dispersed phase, g-mole/ml
$C_{Ad0}$ = initial solute concentration, g-mole/ml
$c_1$ = constant in jet length correlations
$D$ = molecular diffusivity, cm$^2$/s
$D_{AB}^o$ = molecular diffusivity of $A$ in $B$ in very dilute solution, cm$^2$/s
$d_c$ = diameter of the conical section of the extraction column where drop coalescence occurs, cm
$D_d$ = molecular diffusivity of solute in dispersed phase, cm$^2$/s
$d_D$ = diameter of a single free fall drop, cm
$d_f$ = diameter of the drop which would form at the nozzle velocity $U_{nj}$ if a jet did not form, cm
$d_j$ = jet diameter, cm
$d_{jc}$ = jet diameter at breakup, cm
$d_{jm}$ = jet diameter at breakup at maximum area point as estimated from Equations (3) and (4), cm
$d_n$ = nozzle diameter, cm
$d_t$ = tube diameter, cm
$d_1$ = constant in jet length correlations
$E_f$ = fractional extraction
$g$ = acceleration due to gravity, 980 cm/s$^2$
$h_f$ = height of drop free fall, cm
$k_{dj}$, $k_{df}$, $k_{dr}$, $k_{dc}$ = individual dispersed phase coefficients of mass transfer during jetting, drop formation, free fall, and coalescence, cm/s
$k_{df}^*$, $k_{dr}^*$, $k_{dc}^*$ = individual dispersed phase coefficients of mass transfer during drop formation, free fall, and coalescence for low concentration and low transfer rate, cm/s
$(k^*)_{av}$ = mass transfer coefficient for use with arithmetic mean driving force in jet at low concentration and low transfer rate, cm/s
$(k^*)_{lm}$ = mass transfer coefficient for use with logarithmic mean driving force in jet at low concentration and low transfer rate, cm/s
$L_j$ = length of liquid jet, cm
$l_s$ = system length parameter, defined by $\pi\sqrt{\sigma/\Delta\rho g}$
$M_B$ = molecular weight of component $B$, g/g-mole
$(N_D)_{av}$ = average number of free fall drops in the extraction column at any instant
$N_{Oh}$ = Ohnesorge number, defined by $\mu_d/(\rho_c d_n \sigma)^{1/2}$
$N_{Re}$ = Reynolds number, defined by $U_n d_n \rho_d/\mu_d$
$(N_{Re})_{Lj,\max}$ = Reynolds number at maximum jet length, defined by $(U_n)_{Lj,\max} d_n \rho_d/\mu_d$
$N_{Sc}$ = Schmidt number, defined by $\mu_d/\rho_d D_d$
$N_{We}$ = Weber number, defined by $U_n^2 d_n \rho_d/\sigma$
$N_{Wej}$ = Weber number at jetting velocity, defined by $U_{nj}^2 d_n \rho_d/\sigma$
$\Delta N_{We}$, $\Delta N'_{We}$ = modified Weber numbers, defined by $(N_{We} - N_{Wej})$, $(U_n - U_{nj})^2 d_n \rho_d/\sigma$
$Q$ = dispersed phase flow rate, cm$^3$/s
$q$ = rate of extraction, g-mole/s
$Q_c$ = critical dispersed phase flow rate, cm$^3$/s
$r_t$ = average jet radius as a cylindrical tube, cm
$r_1$ = radial distance from origin to jet breakup in spherical coordinates, cm
$r_2$ = radial distance from origin to nozzle tip in spherical coordinates, cm
$T$ = temperature, °K
$t$ = time of free fall, s
$t_e$ = time of exposure to mass transfer, s
$t_f$ = time of drop formation, s
$T_j$, $T_f$, $T_r$, $T_c$ = dimensionless groups, defined by $k_{dj}A_j/Q$, $k_{df}A_f/Q$, $k_{dr}A_r/Q$, and $k_{dc}A_c/Q$
$U_j$ = jet velocity, cm/s
$U_n$ = velocity in nozzle, cm/s
$U_{nj}$ = jetting velocity in nozzle, cm/s
$(U_n)_{Lj,\max}$ = velocity in nozzle at maximum jet length, cm/s
$U_{nm}$ = velocity in nozzle at maximum area point as estimated from Equation (2), cm/s
$U_s$ = slip velocity, cm/s
$V_{bA}$, $V_{bB}$ = molecular volumes of pure components $A$ and $B$ at their normal boiling temperatures, cm$^3$/g-mole
$W$ = rate of extraction, gm/s
$z$ = coordinate (axial position), cm

### Greek Letters

$\alpha$, $\alpha_1$ = constants in jet length correlations
$\delta_m$ = thickness of concentration boundary layer, cm
$\theta_o$ = $\theta$ value for jet surface, rad
$\mu_B$ = viscosity of solvent, cP
$\mu_c$, $\mu_d$ = continuous and dispersed phase viscosities, poise
$\rho_c$, $\rho_d$ = continuous and dispersed phase densities, g/ml
$\Delta\rho$ = density difference, $\rho_d - \rho_c$, g/ml
$\sigma$ = interfacial or surface tension, dyne/cm

## LITERATURE CITED


Burkholder, H. C., and J. C. Berg, "Effect of Mass Transfer on Laminar Jet Breakup. Part I. Liquid Jets in Gases," *AIChE J.*, **20**, 863 (1974).

———, "Effect of Mass Transfer on Laminar Jet Breakup. Part II. Liquid Jets in Liquids," *ibid.*, 872 (1974).

Christiansen, R. M., and A. N. Hixson, "Breakup of a Liquid Jet in a Denser Liquid," *Ind. Eng. Chem.*, **49**, 1017 (1957).

Cobble, M. H., "Nusselt Number for Flow in a Cone," *Trans. ASME, J. Heat Transfer*, 264 (Aug., 1962).

Fisher, R. A., and F. Yates, *Statistical Tables for Biological, Agricultural, and Medical Research*, 6 ed., p. 63, Hafner Publishing Co., New York (1964).

Grant, R. P., and S. Middleman, "Newtonian Jet Stability," *AIChE J.*, **12**, 669 (1966).

Hausen, H., "Verallgemeinerte Potenzbeziehungen fuer den Waermeuebergang in Rahren," *Verfahrenstech. Beih. Z. Ver. dtsch. Ing.*, 4, 91 (1943).

Huang, Y. F., "Mass Transfer during Drop Formation under Jetting Conditions," Ph.D. dissertation, Univ. Kentucky, Lexington (1976).

Johnson, A. I., A. E. Hamielec, D. Ward, and A. Golding, "End Effect Corrections in Heat and Mass Transfer Studies," *Can. J. Chem. Eng.*, 36, 221 (1958).

Keith, F. W., and A. N. Hixson, "Liquid-Liquid Extraction Spray Columns," *Ind. Eng. Chem.*, **47**, 258 (1955).

Lindland, K. P., and S. G. Terjesen, "The Effect of a Surface-Active Agent on Mass Transfer in Falling Drop Extraction," *Chem. Eng. Sci.*, **5**, 1 (1956).
Mayfield, F. W., and W. L. Church, Jr., "Liquid-Liquid Extractor Design," *Ind. Eng. Chem.*, **44**, 2253 (1952).
Meister, B. J., and G. F. Scheele, "Generalized Solution of the Tomotika Stability Analysis for a Cylindrical Jet," *AIChE J.*, **13**, 682 (1967).
———, "Prediction of Jet Length in Immiscible Liquid Systems," *ibid.*, **15**, 689 (1969).
Minhas, S. S., "Dispersed Phase Mass Transfer During Drop Formation and Coalescence in Liquid-Liquid Extraction," Ph.D. dissertation, Univ. Notre Dame, Ind. (1969).
Perry, R. H., C. H. Chilton, and S. D. Kirkpatrick, *Chemical Engineer's Handbook*, 4 ed., McGraw-Hill, New York (1963).
Rayleigh, Lord, "On the Instability of Jets," *Proc. London Math. Soc.*, **10**, 4 (1879).
———, "On the Capillary Phenomena of Jets," *Proc. Royal Soc. (London)*, **29**, 71 (1879).
Reddy, K. A., and L. K. Doraiswamy, "Estimating Liquid Diffusivity," *Ind. Eng. Chem. Fundamentals*, **6**, 77 (1967).
Sawistowski, H., "Influence of Mass-Transfer-Induced Marangoni Effects on Magnitude of Interfacial Area and Equipment Performance in Mass Transfer Operations," *Chem. Ingr. Tech.*, **45**, 1114 (1973).
Scheele, G. F., and B. J. Meister, "Drop Formation at Low Velocities in Liquid-Liquid Systems: Part I. Prediction of Drop Volume. Part II. Prediction of Jetting Velocity," *AIChE J.*, **14**, 9 (1968).
Sherwood, T. K., R. L. Pigford, and C. R. Wilke, *Mass Transfer*, p. 188, McGraw-Hill, New York (1975).
Siemes, W., and J. F. Kauffman, "Tropfenbildung in Flüssigkeiten an Düsen bei hohen Durchsätzen," *Chem. Ingr. Tech.*, **29**, 32 (1957).
Skelland, A. H. P., *Diffusional Mass Transfer*, Chapt. 8, Wiley-Interscience, New York (1974).
———, and W. L. Conger, "A Rate Approach to Design of Perforated-Plate Extraction Columns," *Ind. Eng. Chem. Process Design and Develop.*, **12**, 448 (1973).
Skelland, A. H. P., and K. R. Johnson, "Jet Break-up in Liquid-Liquid Systems," *Can. J. Chem. Eng.*, **52**, 732 (1974).
Skelland, A. H. P., and S. S. Minhas, "Dispersed Phase Mass Transfer during Drop Formation and Coalescence in Liquid-Liquid Extraction," *AIChE J.*, **17**, 1316 (1971).
Skelland, A. H. P., and R. M. Wellek, "Resistance to Mass Transfer inside Droplets," *ibid.*, **10**, 491, 789 (1964).
Smith, S. W. I., and H. Moss, "Experiments with Mercury Jets," *Proc. Royal Soc. (London)*, **A93**, 373 (1917).
Tomotika, S., "On the Instability of a Cylindrical Thread of a Viscous Liquid surrounded by Another Viscous Fluid," *ibid.*, **A150**, 322 (1935).
Treybal, R. E., *Liquid Extraction*, pp. 467-8, McGraw-Hill, New York (1963).
Tyler, E., and E. G. Richardson, "The Characteristic Curves of Liquid Jets," *Proc. Phys. Soc. (London)*, **37**, 297 (1925).
Tyler, E., and F. Watkin, "Experiments with Capillary Jets," *Phil. Mag.*, **14**, 849 (1932).
Vermeulen, T., "Theory for Irreversible and Constant-Pattern Solid Diffusion," *Ind. Eng. Chem.*, **45**, 1664 (1953).
Weber, C., "Disintegration of a Liquid Jet," *Z. Angew Math. Mech.*, **11**, 136 (1931).

*Manuscript received February 17, 1977; revision received May 16, and accepted May 27, 1977.*

# Elongational Flow Behavior of Viscoelastic Liquids:

## Part I. Modeling of Bubble Collapse

**A spherically collapsing gas bubble will create a uniaxial extension of the fluid surrounding it. This flow may be readily analyzed, and it is possible to relate observed experimental parameters such as the pressure inside the bubble and the bubble collapse rate to the predictions of viscoelastic constitutive relations. This study compares the predictions of the Newtonian fluid and a viscoelastic model to observed bubble collapse in three fluids: one Newtonian fluid and two viscoelastic polymer solutions. Good agreement between data and the model was observed for the Newtonian experiments. The viscoelastic solutions, however, yielded rates of collapse which were greater than the Newtonian predictions based on equal zero-shear viscosity. Subsequent modeling with a modified corotational Maxwell fluid yielded good agreement with the data for the transient elongational response in the viscoelastic solutions.**

**GLEN PEARSON**
***and***
**STANLEY MIDDLEMAN**
**Department of Chemical Engineering**
**University of Massachusetts**
**Amherst, Massachusetts 01003**

### SCOPE

The behavior of viscoelastic fluids in elongation is of special importance in such industrial processes as fiber spinning, blow molding, vacuum forming, tubular film extrusion, and certain coating and calendering operations. To date, very little is known about the behavior of viscoelastic fluids in elongation. A particular void exists for fluids of moderate viscosity ($\eta_o \sim 10^2 - 10^4$ *P*) and at high rates of strain ($\dot{\epsilon} > 1\ s^{-1}$).

Correspondence concerning this paper should be addressed to Stanley Middleman. Glen Pearson is with Eastman Kodak Company, Rochester, New York 14650.